10-25-2017

Responsive Nanogel Probe for Ratiometric Fluorescent Sensing of pH and Strain in Hydrogels

Mingning Zhu
University of Manchester

Dongdong Lu
University of Manchester

Shanglin Wu
University of Manchester

Qing Lian
University of Manchester

Wenkai Wang
University of Manchester

See next page for additional authors

Recommended Citation
Zhu, M.; Lu, D.; Wu, S.; Lian, Q.; Wang, W.; Milani, A.H.; Cui, Z.; Nguyen, N.T.; Chen, M.; Lyon, L.A.; Adlam, D.J.; Freemont, A.J.; Hoyland, J.A.; Saunders, B.R. Responsive Nanogel Probe for Ratiometric Fluorescent Sensing of pH and Strain in Hydrogels. *ACS Macro Lett.* **2017**, *6*, 1245-1250.
doi: 10.1021/acsmacrolett.7b00709

Responsive Nanogel Probe for Ratiometric Fluorescent Sensing of pH and Strain in Hydrogels

Authors
Mingning Zhu, Dongdong Lu, Shanglin Wu, Qing Lian, Wenkai Wang, Amir H. Milani, Zhengxing Cui, Nam T. Nguyen, Mu Chen, L. Andrew Lyon, Daman J. Adlam, Anthony J. Freemont, Judith A. Hoyland, and Brian R. Saunders

ACS Macro Letters

Letter

pubs.acs.org/macroletters

Responsive Nanogel Probe for Ratiometric Fluorescent Sensing of pH and Strain in Hydrogels

Mingning Zhu,[†] Dongdong Lu,[†] Shanglin Wu,[†] Qing Lian,[†] Wenkai Wang,[†] Amir H. Milani,[†] Zhengxing Cui,[†] Nam T. Nguyen,[†] Mu Chen,[†] L. Andrew Lyon,[‡] Daman J. Adlam,[§] Anthony J. Freemont,[§,∥] Judith A. Hoyland,[§,∥] and Brian R. Saunders*[,†]

[†]School of Materials, University of Manchester, MSS Tower, Manchester M13 9PL, U.K.

[‡]Schmid College of Science and Technology, Chapman University, Orange, California 92866, United States

[§]Division of Cell Matrix Biology and Regenerative Medicine, Faculty of Biology, Medicine and Health, University of Manchester, Oxford Road, Manchester M13 9PT, U.K.

[∥]NIHR Manchester Musculoskeletal Biomedical Research Unit, Central Manchester Foundation Trust, Manchester Academic Health Science Centre, Manchester, U.K.

Supporting Information

ABSTRACT: In this study a new pH-responsive nanogel probe containing a complementary nonradiative resonance energy transfer (NRET) fluorophore pair is investigated and its ability to act as a versatile probe of network-related changes in three hydrogels demonstrated. Fluorescent sensing using NRET is a powerful method for studying relationships between Angstrom length-scale structure and macroscopic properties of soft matter. Unfortunately, inclusion of NRET fluorophores into such materials requires material-specific chemistry. Here, low concentrations of preformed nanogel probes were included into hydrogel hosts. Ratiometric photoluminescence (PL) data for the gels labeled with the nanogel probes enabled pH-triggered swelling and deswelling to be studied as well as Ca^{2+}-triggered collapse and solute release. PL measurements during compression of a nanogel probe-labeled nanocomposite gel demonstrated mechanochromic behavior and strain sensing. The new nanogel probes have excellent potential for investigating the internal structures of gels and provide a versatile ratiometric fluorescent platform for studying pH and strain.

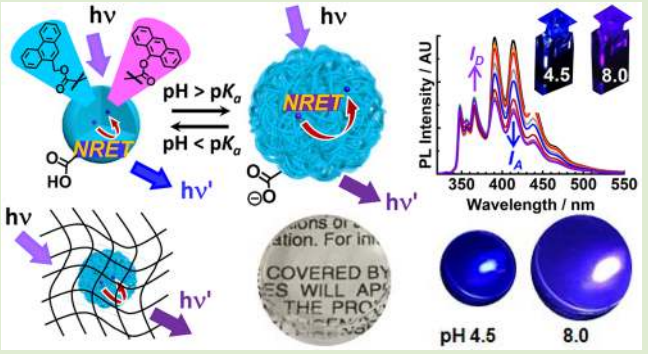

Hydrogels[1−7] are one of the most actively studied classes of soft matter due to their excellent potential for applications involving drug delivery,[3] sensing,[8] biological function mimicry,[9] regenerative medicine,[10] water purification,[11] and optical switching.[12] Well-studied conventional hydrogels include those based on polyethylene glycol[13] and polyamides.[14,15] However, conventional gels are intrinsically brittle due to a nonuniform distribution of elastically effective chain lengths. To overcome this problem high ductility gels (with greater structural complexity) were introduced such as a double network,[5] nanocomposite,[16,17] slide ring,[18] and doubly cross-linked gels.[19] While gel swelling behaviors and mechanical properties are well understood,[6] the internal structures of gels can be challenging to study. Understanding the internal structure is especially important for gels with complex structures.[5,16,17,19] Hence, improving the understanding of the relationship between the internal structure of gels and macroscopic gel properties is a key challenge for polymer and biomaterials science.[20] Techniques typically used to address this challenge involve small-angle scattering[21] and SEM.[22] However, these techniques either require expensive equipment and large facilities (e.g., synchrotrons) or may introduce artifacts. Here, we report an alternative and versatile approach for studying the internal structure and environment in gels. We introduce new pH-responsive nanogel probe particles and show that they can be used to fluorescently sense the local environment (e.g., pH) and structural changes (e.g., local network collapse) in three different "host" hydrogels. The nanogel probe is easily constructed and small (<50 nm diameter) with relatively bright photoluminescence (PL) intensity. The nanogel probe is cytocompatible and robust and can innocuously probe the internal structure of gels and sense changes with high fidelity.

The nanogels studied here are cross-linked polymer colloid nanoparticles with titratable −COOH groups. The nanogels swell due to $-COO^-$ formation which become dominant when the pH exceeds the apparent pK_a.[23] The nanogel probes

Received: September 12, 2017
Accepted: October 19, 2017
Published: October 25, 2017

DOI: 10.1021/acsmacrolett.7b00709
ACS Macro Lett. 2017, 6, 1245−1250

Scheme 1. (a) pH-Responsive Nanogel Probes ($NG_{Ph/An}$) and Small Amounts of $NG_{Ph/An}$ Were Included within (b) a Doubly Cross-Linked Nanogel (DX NG), (c) a Poly(acrylamide) Gel, and (d) a Nanocomposite Gel[a]

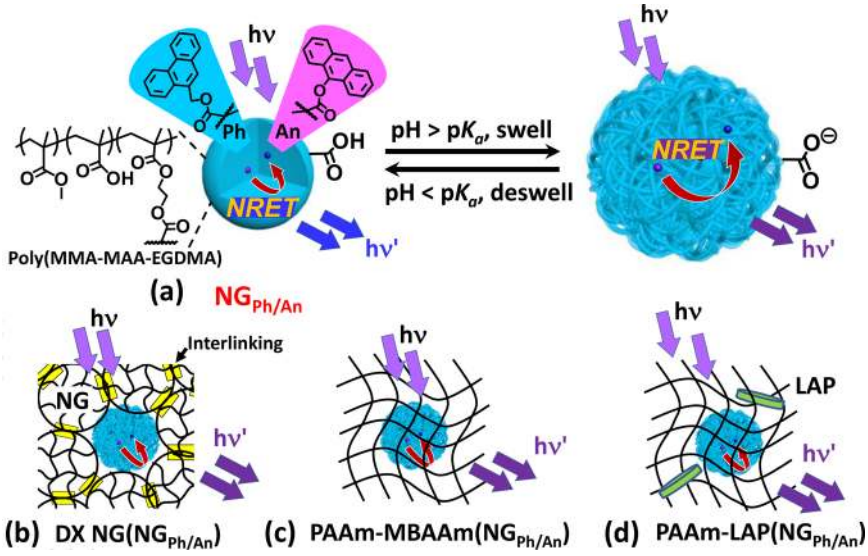

[a]MBAAm and LAP are *N,N′*-methylenebis(acrylamide) and laponite RD, respectively.

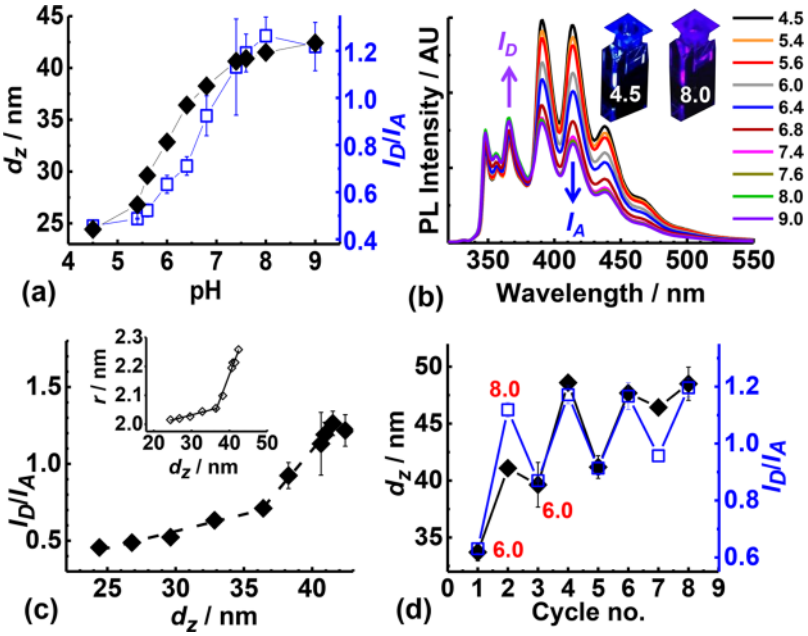

Figure 1. (a) Variation of *z*-average diameter (d_z) and PL intensity ratio of the donor and acceptor peaks (I_D/I_A) with pH for an $NG_{Ph/An}$ dispersion. (b) PL spectra for the $NG_{Ph/An}$ dispersions. The inset shows cuvettes of the dispersions irradiated with UV light. The pH values are shown. (c) Variation of I_D/I_A with d_z. The inset shows the calculated average separation between the Ph and An. (d) Data from repeated cycling between pH 6.0 and 8.0.

($NG_{Ph/An}$, Scheme 1a) were prepared by copolymerization of methyl methacryate (MMA), methacrylic acid (MAA), ethylene glycol dimethacrylate (EGDMA), (9-phenanthryl)methyl methacrylate (Ph), and (9-anthryl)methacrylate (An). Ph (donor) and An (acceptor) are complementary nonresonance energy transfer (NRET) pairs. NRET is a nonradiative and distance-dependent energy transfer process that occurs between a photoexcited fluorophore (donor) and a ground-state fluorophore (acceptor).[24,25] Energy transfer can occur via dipole-induced dipole coupling when the donor emission and acceptor absorption overlap which enables use as a spectroscopic ruler.[26] We hypothesized that incorporation of a complementary NRET fluorophore pair into a pH-responsive nanogel particle would provide a preformed nanoprobe that could sense the internal pH or strain within a "host" macroscopic gel. In contrast to earlier temperature-responsive microgels containing Ph and An[24] the new nanogel probe particles reported here were pH responsive.

Scheme 1b–d depicts the three hydrogel "hosts" studied. We assembled pH-responsive hydrogels of covalently interlinked (nonlabeled) nanogel particles[23] (Scheme 1b) and used $NG_{Ph/An}$ to sense pH and gel collapse. These gels contained *intra-* and *inter*-cross-linked poly(MMA-MAA-EGDMA) nanogel particles and are termed doubly cross-linked nanogels (DX

DOI: 10.1021/acsmacrolett.7b00709
ACS Macro Lett. 2017, 6, 1245−1250

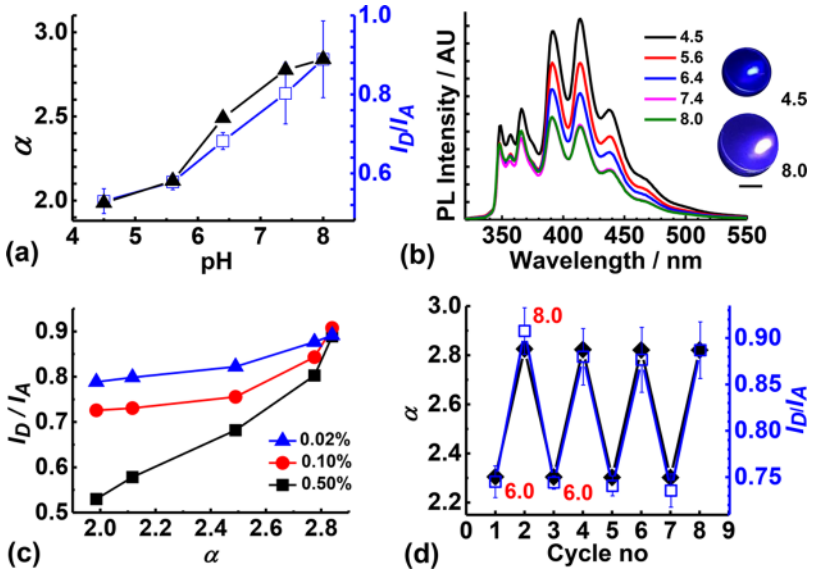

Figure 2. (a) Variation of the average linear swelling ratio (α) and I_D/I_A with pH for DX NG($NG_{Ph/An}$)$_{0.50}$. (b) PL spectra for DX NG($NG_{Ph/An}$)$_{0.50}$. The inset shows the gel images obtained with UV light. Scale bar: 10 mm. (c) Variation of I_D/I_A with α for DX NG($NG_{Ph/An}$)$_x$ gels (x values are shown). (d) Data obtained for the gels by cycling the pH between 6.0 and 8.0.

NGs).[27] They have potential application as an injectable gel for intervertebral disc (IVD) repair.[28] The $NG_{Ph/An}$ probes were also included during synthesis of poly(acrylamide) (PAAm) hydrogel (Scheme 1c) and a tough nanocomposite gel (Scheme 1d).

The nanogel probe particles ($NG_{Ph/An}$) were synthesized using emulsion polymerization (Supporting Information) and were pH-responsive. They had an average diameter of 16 nm based on TEM (Figures S3a and Table S2). The particles contained Ph (0.42 mol %) and An (0.59 mol %) as determined by UV−visible spectroscopy (see Figure S2) and swelled when the pH increased beyond 5.4 (Figure 1a) (see Supporting Information for other characterization data.) The PL spectra obtained from the $NG_{Ph/An}$ dispersions were highly sensitive to pH (Figure 1b). As the pH increased from 4.5 to 9.0 the intensity of the Ph donor band (I_D) at 366 nm increased, whereas the intensity of the An acceptor band (I_A) at 414 nm decreased. Furthermore, the $NG_{Ph/An}$ dispersion changed from blue to violet when illuminated with UV light (Figure 1b, inset). The I_D/I_A ratio increased with increasing pH (Figure 1a) because of decreased resonance energy transfer between Ph and An due to their increased separation as a consequence of particle swelling. PL spectra for control of NG_{Ph} and NG_{An} dispersions (Figure S7) confirmed that the I_{366}/I_{414} ratio could *only* be used for ratiometric detection when the nanogel particles contained *both* Ph and An (Figure S8). The quantum yield at pH 8.0 for the $NG_{Ph/An}$ particles was 13%, which indicates that the nanoprobes had a reasonably bright PL emission.[29] The ability of fluorescent nanogel probes to report pH and/or strain in load-bearing tissue is potentially important for future biomaterial applications.[30] The $NG_{Ph/An}$ particles were not cytotoxic as judged by cell challenge data obtained using human nucleus pulposus (NP) cells and a $NG_{Ph/An}$ concentration that was high enough for well-resolved PL spectra to be recorded (Figure S9).

The I_D/I_A ratio increase that is apparent with increasing pH (Figure 1a) occurred *after* the increase of the d_z values. This result indicates that the PL and DLS data originated from *different* particle regions. A plot of I_D/I_A against d_z (Figure 1c) shows two linear regions with a discontinuity at $d_z \sim 36$ nm. NRET efficiencies calculated from the PL spectra for $NG_{Ph/An}$ and NG_{Ph} (Figure S7) enabled calculation of the average donor−acceptor distance (r) (see Supporting Information). Figure 1c (inset) shows the variation of r with d_z. A linear relationship between r and d_z can be expected if nanoscale and macroscale swelling follow affine swelling.[31] We ascribe the two linear regions that are evident to two-stage nanogel swelling. This behavior is likely due to shell swelling at lower pH values and core swelling at higher pH. Electrophoretic mobility data (Figure S5) support this new structural insight for nanogels (see additional core−shell $NG_{Ph/An}$ discussion in the Supporting Information). The reversibility of the I_D/I_A changes was probed by cycling the dispersion pH between 6.0 and 8.0 (Figure 1d). While the I_D/I_A ratios showed reversibility after the first cycle, the dispersions began to aggregate slightly due to the increased ionic strength associated with buffer changing. The fact that the I_D/I_A values were *not significantly affected by dispersion aggregation* is potentially advantageous for future nanogel probe applications. The effects of added Ca^{2+} on I_D/I_A and d_z for an $NG_{Ph/An}$ dispersion at pH 9.0 were also studied (Figure S10). The I_D/I_A ratio decreased at concentrations of 0.020 M or more and stabilized at 0.57. This result shows that particle collapse occurred (from Figure 1a). However, the d_z values *increased* due to aggregation because of electrostatic screening and ionic cross-linking.[32] These two examples demonstrate that ratiometric PL intensity data enabled study of $NG_{Ph/An}$ particle size in conditions where DLS was not suitable. The stability of both the d_z and I_D/I_A values for the $NG_{Ph/An}$ nanoprobes as a function of time was investigated at selected pH values in the range of 4.5−10.8 (Figure S11). The d_z and I_D/I_A values changed by an average of less than 10% over a 10 day period and demonstrated good stability.

We investigated the ability of $NG_{Ph/An}$ to act as a nanogel probe for swelling/deswelling transitions within an injectable pH-responsive DX NG gel (Scheme 1b). This injectable gel was assembled from swollen vinyl-functionalized poly(MMA-MAA-EGDMA) NG particles[27] and very small proportions of $NG_{Ph/An}$ particles (ranging from 0.02 to 0.50%) as depicted in

DOI: 10.1021/acsmacrolett.7b00709
ACS Macro Lett. 2017, 6, 1245−1250

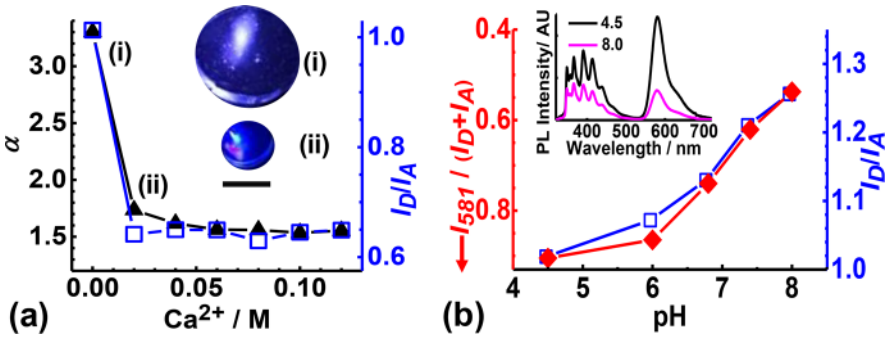

Figure 3. (a) Effect of added $CaCl_2$ on α and I_D/I_A for DX NG$(NG_{Ph/An})_{0.10}$. The pH was 8.9. The gel images were obtained using UV light. Scale bar: 10 mm. (b) Variation of $I_{581}/(I_D + I_A)$ and I_D/I_A with pH for DX NG$(NG_{Ph/An})_{0.10}$ containing RBITC. The inset shows the PL spectra for the gel at pH 4.5 and 8.0.

Scheme S1c. The viscous dispersions transformed into elastic gels due to inter-NG linking via free-radical coupling of the pendent vinyl groups. These DX NG$(NG_{Ph/An})_x$ gels contained less than one $NG_{Ph/An}$ probe particle per 20 covalently interlinked NG matrix particles and were transparent in visible light (Figure S12). The average linear swelling ratio ($\alpha = Q^{1/3}$, where Q is the volume swelling ratio) for the DX NG$(NG_{Ph/An})_{0.50}$ gels increased as the pH increased (Figure 2a) due to swelling of the constituent NG particles (Figure 1a). PL spectra for the gels were pH-dependent (Figure 2b). The I_D/I_A ratio *increased* with increasing pH due to gel swelling. Additionally, the pH increase caused the gels to change from blue to violet (Figure 2b, inset). These results show that pH-triggered swelling of the $NG_{Ph/An}$ particles occurred within the DX NG$(NG_{Ph/An})_{0.50}$ gel. Because the $NG_{Ph/An}$ particles did not alter the pH-dependent α values significantly (Figure S13), they behaved as innocuous probes. The latter result is potentially beneficial for future gel studies.

The intensity of the DX NG$(NG_{Ph/An})_x$ PL spectra (Figure S14) and I_D/I_A fidelity (Figure 2c) increased with increasing x. The latter trend is due to the increased dominance of the NRET-based I_D and I_A changes compared to the PL intensity changes associated with pH-dependent light scattering from the DX NG matrix. The minimum I_D/I_A ratio of 0.53 corresponded to almost complete collapse from comparison with the ratiometric PL data for dispersed $NG_{Ph/An}$ (Figure 1a). Cyclic gel swelling studies were also conducted between pH 6.0 and 8.0 (Figure 2d) which demonstrated excellent reversibility of the I_D/I_A (and α) response. Hence, the *nanogel probes successfully reported gel swelling/deswelling.*

The nanogel probe was able to report collapse of a DX NG$(NG_{Ph/An})_{0.10}$ gel due to Ca^{2+} (Figure 3a) (see Figure S15 for the PL spectra.) A major decrease of α and I_D/I_A occurred for Ca^{2+} concentrations of 0.020 M or higher due to electrostatic screening and ionic cross-linking of the COO^- groups by Ca^{2+}. Comparing the minimum I_D/I_A and α values to those shown in Figure 2c (x = 0.10) shows that more pronounced gel deswelling was caused by Ca^{2+} (at pH 8.9) than occurred in its absence at pH 4.5. This result demonstrates the ability of Ca^{2+} to extinguish electrostatic repulsion.

The nanogel probe also enabled simultaneous monitoring of pH-triggered swelling and solute release. For this study DX NG$(NG_{Ph/An})_{0.10}$ gel was prepared containing RBITC (structure shown in Figure S16f). The latter model solute has an emission maximum at 581 nm (Figure S16b). Figure 3b shows the pH-triggered changes of the relative PL intensity for RBITC ($I_{581}/(I_D + I_A)$) from the RBITC-loaded DX NG-$(NG_{Ph/An})_{0.10}$ gel. The $I_{581}/(I_D + I_A)$ value *decrease* (from RBITC release) closely followed the I_D/I_A ratio *increase* (due to gel swelling). (Figure S16 of the Supporting Information shows the spectra, calibration, and release data.) Because this family of injectable gels has potential application for IVD repair,[28] we studied its mechanical properties using uniaxial compression (Figure S17). The modulus and yield strain were 19 kPa and 47%, respectively (Table S3). The former value is comparable to the complex modulus reported for human NPs.[33] The DX NG$(NG_{Ph/An})_{0.10}$ gel was not cytotoxic to NP cells (Figure S18). These data demonstrate the ability of using $NG_{Ph/An}$ to *simultaneously monitor solute release and swelling/deswelling changes* of an injectable pH-responsive gel with potential biomaterial use.

The ability of $NG_{Ph/An}$ particles to act as a probe within a conventional (non-pH-responsive) PAAm-MBAAm gel (Scheme 1c) was investigated. The gel was prepared by free-radical solution polymerization at pH 5.6 in the presence of a low concentration of $NG_{Ph/An}$ (see Supporting Information). The minimum I_D/I_A ratio of 0.51 (Figure 4a) matches that

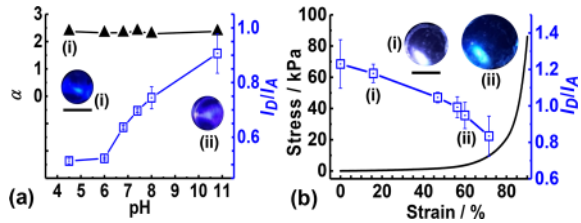

Figure 4. (a) Effect of pH on α and I_D/I_A for PAAm-MBAAm-$(NG_{Ph/An})_{0.10}$ gel. (b) Variation of stress and I_D/I_A with strain for a PAAm-LAP$(NG_{Ph/An})_{0.03}$ nanocomposite gel. The gel images were obtained in UV light. Scale bar: 10 mm.

shown in Figure 1a and confirms the nanogel probes were collapsed. As the pH of the PAAm$(NG_{Ph/An})_{0.10}$ gel increased the I_D/I_A ratio also increased and reached 0.91 at pH 10.8 (Figure S19 shows the PL spectra). This value corresponds to d_z = 38 nm (Figure 1c) and implies that the particles did not fully swell. We attribute this behavior to physical constraint of the nanogel probe particles by the PAAm-MBAAm matrix. Nevertheless, the PL changes were sufficiently strong for the gel to change from blue to violet as the pH increased (Figure 4a). Because the α values confirm this gel did not change its swelling with pH (as expected) the nanogel probe signal was decoupled from the gel swelling. Images of these gels containing universal indicator (Figure S20) confirm that the internal pH values of

DOI: 10.1021/acsmacrolett.7b00709
ACS Macro Lett. 2017, 6, 1245−1250

the gels matched those of the buffer solutions. Hence, $NG_{Ph/An}$ *reported the internal gel pH*.

A low concentration of $NG_{Ph/An}$ particles (0.03 wt %) was included during the preparation of a tough PAAm-LAP nanocomposite gel (Scheme 1d). The gel was synthesized by free-radical polymerization of AAm in the presence of LAP which acted as a cross-linker.[16] The PAAm-LAP ($(NG_{Ph/An})_{0.03}$) gel changed from violet to blue when compressed and was mechanochromic (inset of Figure 4b) (Figure S21 shows the PL spectra). The high gel pH (10.7) and absence of an organic cross-linker, such as MBAAm, ensured the $NG_{Ph/An}$ particles swelled fully prior to deformation. The I_D/I_A ratio decreased from 1.25 to 0.85 as the macroscopic strain increased from 0% to 72%. These I_D/I_A values correspond to spherical equivalent d_z values of 41 and 38 nm, respectively, from Figure 1c and demonstrate for the first time the ability of nanoprobe gel particles to *act as a strain sensor* within a gel to the best of our knowledge.

This study has introduced a versatile pH-responsive nanogel probe particle ($NG_{Ph/An}$) which, when included into three host gels, enabled ratiometric sensing of either internal pH, gel collapse, or both as well as Ca^{2+}, pH-triggered release of a fluorescent solute or strain. The ratiometric PL response could be tuned using nanogel probe concentration, and the changes due to pH were reversible. This new approach to conferring ratiometric sensing properties to gels required only nanogel probes dispersed in the reactant mixture used to construct the gels and should therefore be generally applicable. The $NG_{Ph/An}$ particles enabled ratiometric PL intensity detection at very low concentrations and have good potential to act as innocuous probes for studying internal structures, pH, and swelling for other hydrogels. The construction approach used for the nanogel probes should also be suitable for other NRET pairs. Furthermore, nanogel probes loaded into DX NG gels, or other injectable gels, may lead to load-supporting gels with built-in fluorescent strain reporting for next-generation biomaterials.

■ ASSOCIATED CONTENT

Supporting Information

The Supporting Information is available free of charge on the ACS Publications website at DOI: 10.1021/acsmacrolett.7b00709.

Experimental details, synthesis schemes, additional discussions, and characterization data (PDF)

■ AUTHOR INFORMATION

Corresponding Author

*Brian R. Saunders: brian.saunders@manchester.ac.uk.

ORCID

Brian R. Saunders: 0000-0003-1410-2967

Notes

The authors declare no competing financial interest.

■ ACKNOWLEDGMENTS

This work was supported by a 5 year EPSRC Established Career Fellowship awarded to BRS (M002020/1).

■ REFERENCES

(1) Azevedo, S.; Costa, A. M. S.; Andersen, A.; Choi, I. S.; Birkedal, H.; Mano, J. F. Bioinspired Ultratough Hydrogel with Fast Recovery, Self-Healing, Injectability and Cytocompatibility. *Adv. Mater.* **2017**, *29*, 1700759.

(2) Kloxin, A. M.; Kasko, A. M.; Salinas, C. N.; Anseth, K. S. Photodegradable Hydrogels for Dynamic Tuning of Physical and Chemical Properties. *Science* **2009**, *324*, 59−63.

(3) Langer, R.; Tirrell, D. A. Designing materials for biology and medicine. *Nature* **2004**, *428*, 487−492.

(4) Lutolf, M. P.; Hubbell, J. A. Synthetic biomaterials as instructive extracellular microenvironments for morphogenesis in tissue engineering. *Nat. Biotechnol.* **2005**, *23*, 47−55.

(5) Nonoyama, T.; Wada, S.; Kiyama, R.; Kitamura, N.; Mredha, M. T. I.; Zhang, X.; Kurokawa, T.; Nakajima, T.; Takagi, Y.; Yasuda, K.; Gong, J. P. Double-Network Hydrogels Strongly Bondable to Bones by Spontaneous Osteogenesis Penetration. *Adv. Mater.* **2016**, *28*, 6740−6745.

(6) Peppas, N. A.; Hilt, J. Z.; Khademhosseini, A.; Langer, R. Hydrogels in Biology and Medicine: From Molecular Principles to Bionanotechnology. *Adv. Mater.* **2006**, *18*, 1345−1360.

(7) Xing, R.; Liu, K.; Jiao, T.; Zhang, N.; Ma, K.; Zhang, R.; Zou, Q.; Ma, G.; Yan, X. An Injectable Self-Assembling Collagen−Gold Hybrid Hydrogel for Combinatorial Antitumor Photothermal/Photodynamic Therapy. *Adv. Mater.* **2016**, *28*, 3669−3676.

(8) Thornton, P. D.; Mart, R. J.; Ulijn, R. V. Enzyme-Responsive Polymer Hydrogel Particles for Controlled Release. *Adv. Mater.* **2007**, *19*, 1252−1256.

(9) Green, J. J.; Elisseeff, J. H. Mimicking biological functionality with polymers for biomedical applications. *Nature* **2016**, *540*, 386−394.

(10) Wu, Y.; Wang, L.; Guo, B.; Ma, P. X. Interwoven Aligned Conductive Nanofiber Yarn/Hydrogel Composite Scaffolds for Engineered 3D Cardiac Anisotropy. *ACS Nano* **2017**, *11*, 5646−5659.

(11) Chen, Y.; Chen, L.; Bai, H.; Li, L. Graphene oxide-chitosan composite hydrogels as broad-spectrum adsorbents for water purification. *J. Mater. Chem. A* **2013**, *1*, 1992−2001.

(12) Lee, H. Y.; Cai, Y.; Bi, S.; Liang, Y. N.; Song, Y.; Hu, X. M.; Dual-Responsive, A. Nanocomposite toward Climate-Adaptable Solar Modulation for Energy-Saving Smart Windows. *ACS Appl. Mater. Interfaces* **2017**, *9*, 6054−6063.

(13) Lin, C.-C.; Anseth, K. S. PEG Hydrogels for the Controlled Release of Biomolecules in Regenerative Medicine. *Pharm. Res.* **2009**, *26*, 631−643.

(14) Durmaz, S.; Okay, O. Acrylamide/2-acrylamido-2-methylpropane sulfonic acid sodium salt-based hydrogels: synthesis and characterization. *Polymer* **2000**, *41*, 3693−3704.

(15) Pehlivaner Kara, M. O.; Ekenseair, A. K. Free Epoxide Content Mediates Encapsulated Cell Viability and Activity through Protein Interactions in a Thermoresponsive, In Situ Forming Hydrogel. *Biomacromolecules* **2017**, *18*, 1473−1481.

(16) Haraguchi, K.; Takehisa, T. Nanocomposite Hydrogels: A Unique Organic−Inorganic Network Structure with Extraordinary Mechanical, Optical, and Swelling/De-swelling Properties. *Adv. Mater.* **2002**, *14*, 1120−1124.

(17) Unterman, S.; Charles, L. F.; Strecker, S. E.; Kramarenko, D.; Pivovarchik, D.; Edelman, E. R.; Artzi, N. Hydrogel Nanocomposites with Independently Tunable Rheology and Mechanics. *ACS Nano* **2017**, *11*, 2598−2610.

(18) Bin Imran, A.; Esaki, K.; Gotoh, H.; Seki, T.; Ito, K.; Sakai, Y.; Takeoka, Y. Extremely stretchable thermosensitive hydrogels by introducing slide-ring polyrotaxane cross-linkers and ionic groups into the polymer network. *Nat. Commun.* **2014**, *5*, 5124.

(19) Zhu, L.; Qiu, J.; Sakai, E.; Ito, K. Rapid Recovery Double Cross-Linking Hydrogel with Stable Mechanical Properties and High Resilience Triggered by Visible Light. *ACS Appl. Mater. Interfaces* **2017**, *9*, 13593−13601.

(20) Storm, C.; Pastore, J. J.; MacKintosh, F. C.; Lubensky, T. C.; Janmey, P. A. Nonlinear elasticity in biological gels. *Nature* **2005**, *435*, 191−194.

(21) Hu, Z.; Chen, L.; Betts, D. E.; Pandya, A.; Hillmyer, M. A.; DeSimone, J. M. Optically Transparent, Amphiphilic Networks Based on Blends of Perfluoropolyethers and Poly(ethylene glycol). *J. Am. Chem. Soc.* **2008**, *130*, 14244−14252.

DOI: 10.1021/acsmacrolett.7b00709
ACS Macro Lett. 2017, 6, 1245−1250

(22) Trappmann, B.; Gautrot, J. E.; Connelly, J. T.; Strange, D. G. T.; Li, Y.; Oyen, M. L.; Cohen Stuart, M. A.; Boehm, H.; Li, B.; Vogel, V.; Spatz, J. P.; Watt, F. M.; Huck, W. T. S. Extracellular-matrix tethering regulates stem-cell fate. *Nat. Mater.* **2012**, *11*, 642−649.
(23) Milani, A. H.; Fielding, L. A.; Greensmith, P.; Saunders, B. R.; Adlam, D. J.; Freemont, A. J.; Hoyland, J. A.; Hodson, N. W.; Elsawy, M. A.; Miller, A. F.; Ratcliffe, L. P. D.; Mykhaylyk, O. O.; Armes, S. P. Anisotropic pH-Responsive Hydrogels Containing Soft or Hard Rod-Like Particles Assembled Using Low Shear. *Chem. Mater.* **2017**, *29*, 3100−3110.
(24) Gan, D. J.; Lyon, L. A. Interfacial nonradiative energy transfer in responsive core-shell hydrogel nanoparticles. *J. Am. Chem. Soc.* **2001**, *123*, 8203−8209.
(25) Ryu, J.-H.; Chacko, R. T.; Jiwpanich, S.; Bickerton, S.; Babu, R. P.; Thayumanavan, S. Self-Cross-Linked Polymer Nanogels: A Versatile Nanoscopic Drug Delivery Platform. *J. Am. Chem. Soc.* **2010**, *132*, 17227−17235.
(26) Ray, P. C.; Fan, Z.; Crouch, R. A.; Sinha, S. S.; Pramanik, A. Nanoscopic optical rulers beyond the FRET distance limit: fundamentals and applications. *Chem. Soc. Rev.* **2014**, *43*, 6370−6404.
(27) Milani, A. H.; Saunders, J. M.; Nguyen, N. T.; Ratcliffe, L. P. D.; Adlam, D. J.; Freemont, A. J.; Hoyland, J. A.; Armes, S. P.; Saunders, B. R. Synthesis of polyacid nanogels: pH-responsive sub-100 nm particles for functionalisation and fluorescent hydrogel assembly. *Soft Matter* **2017**, *13*, 1554−1560.
(28) Milani, A. H.; Freemont, A. J.; Hoyland, J. A.; Adlam, D. J.; Saunders, B. R. Injectable Doubly Cross-Linked Microgels for Improving the Mechanical Properties of Degenerated Intervertebral Discs. *Biomacromolecules* **2012**, *13*, 2793−2801.
(29) Talanov, V. S.; Regino, C. A. S.; Kobayashi, H.; Bernardo, M.; Choyke, P. L.; Brechbiel, M. W. Dendrimer-Based Nanoprobe for Dual Modality Magnetic Resonance and Fluorescence Imaging. *Nano Lett.* **2006**, *6*, 1459−1463.
(30) Fitch, K. R.; Goodwin, A. P. Mechanochemical Reaction Cascade for Sensitive Detection of Covalent Bond Breakage in Hydrogels. *Chem. Mater.* **2014**, *26*, 6771−6776.
(31) Rubinstein, M.; Colby, R. H.; Dobrynin, A. V.; Joanny, J.-F. Elastic Modulus and Equilibrium Swelling of Polyelectrolyte Gels. *Macromolecules* **1996**, *29*, 398−406.
(32) Papageorgiou, S. K.; Kouvelos, E. P.; Favvas, E. P.; Sapalidis, A. A.; Romanos, G. E.; Katsaros, F. K. Metal−carboxylate interactions in metal−alginate complexes studied with FTIR spectroscopy. *Carbohydr. Res.* **2010**, *345*, 469−473.
(33) Iatridis, J. C.; Weidenbaum, M.; Setton, L. A.; Mow, V. C. Is the Nucleus Pulposus a Solid or a Fluid? Mechanical Behaviors of the Nucleus Pulposus of the Human Intervertebral Disc. *Spine* **1996**, *21*, 1174−1184.

DOI: 10.1021/acsmacrolett.7b00709
ACS Macro Lett. 2017, 6, 1245−1250